All-polymer solar cells with over 16% efficiency and enhanced stability enabled by compatible solvent and polymer additives

Received: 22 February 2021 | Revised: 27 March 2021 | Accepted: 12 April 2021

DOI: 10.1002/agt2.58

Aggregate WILEY Open Access

RESEARCH ARTICLE

All-polymer solar cells with over 16% efficiency and enhanced stability enabled by compatible solvent and polymer additives

Ruijie Ma[1,7,#] | **Jianwei Yu**[3,#] | **Tao Liu**[1,7] | **Guangye Zhang**[4] | **Yiqun Xiao**[5] | **Zhenghui Luo**[1,7] | **Gaoda Chai**[1] | **Yuzhong Chen**[1,7] | **Qunping Fan**[6] | **Wenyan Su**[6,10] | **Gang Li**[2] | **Ergang Wang**[6,9] | **Xinhui Lu**[5] | **Feng Gao**[3] | **Bo Tang**[2] | **He Yan**[1,7,8]

[1] Department of Chemistry, Guangdong-Hong Kong-Macao Joint Laboratory of Optoelectronic and Magnetic Functional Materials, Energy Institute and Hong Kong Branch of Chinese National Engineering Research Center for Tissue Restoration and Reconstruction, Hong Kong University of Science and Technology, Kowloon, Hong Kong, China

[2] College of Chemistry, Chemical Engineering and Materials Science, Key Laboratory of Molecular and Nano Probes, Ministry of Education, Collaborative Innovation Center of Functionalized Probes for Chemical Imaging in Universities of Shandong, Institute of Materials and Clean Energy, Shandong Provincial Key Laboratory of Clean Production of Fine Chemicals, Shandong Normal University, Jinan, China

[3] Department of Physics, Chemistry and Biology (IFM), Linköping University, Linköping, Sweden

[4] College of New Materials and New Energies, Shenzhen Technology University, Shenzhen, China

[5] Department of Physics, Chinese University of Hong Kong, New Territories, Hong Kong, China

[6] Department of Chemistry and Chemical Engineering, Chalmers University of Technology, Göteborg, Sweden

[7] Hong Kong University of Science and Technology-Shenzhen Research Institute, Nanshan, Shenzhen, P. R. China

[8] State Key Laboratory of Luminescent Materials and Devices, Institute of Polymer Optoelectronic Materials and DevicesSouth China University of Technology (SCUT), Guangzhou, P. R. China

[9] School of Materials Science and Engineering, Zhengzhou University, Zhengzhou, China

[10] Guangdong Provincial Key Laboratory of Optical Fiber Sensing and Communications, Siyuan Laboratory, Department of Physics, Jinan University, Guangzhou, China

Correspondence

Bo Tang, College of Chemistry, Chemical Engineering and Materials Science, Key Laboratory of Molecular and Nano Probes, Ministry of Education, Collaborative Innovation Center of Functionalized Probes for Chemical Imaging in Universities of Shandong, Institute of Materials and Clean Energy, Shandong Provincial Key Laboratory of Clean Production of Fine Chemicals, Shandong Normal University, Jinan 250014, China.
Email: tangb@sdnu.edu.cn

Tao Liu and He Yan, Department of Chemistry, Guangdong-Hong Kong-Macao Joint Laboratory of Optoelectronic and Magnetic Functional Materials, Energy Institute and Hong Kong Branch of Chinese National Engineering Research Center for Tissue Restoration and Reconstruction, Hong Kong University of Science and Technology, Clear Water Bay, Kowloon, Hong Kong, China.
Email: liutaozhx@ust.hk; hyan@ust.hk

Guangye Zhang, College of New Materials and New Energies, Shenzhen Technology University, Shenzhen, China.
Email: zhangguangye@sztu.edu.cn

Feng Gao, Department of Physics, Chemistry and Biology (IFM), Linköping University, Linköping SE-58183, Sweden.
Email: feng.gao@liu.se

[#]Both the authors contributed equally to this manuscript.

Abstract

Considering the robust and stable nature of the active layers, advancing the power conversion efficiency (PCE) has long been the priority for all-polymer solar cells (all-PSCs). Despite the recent surge of PCE, the photovoltaic parameters of the state-of-the-art all-PSC still lag those of the polymer:small molecule-based devices. To compete with the counterparts, judicious modulation of the morphology and thus the device electrical properties are needed. It is difficult to improve all the parameters concurrently for the all-PSCs with advanced efficiency, and one increase is typically accompanied by the drop of the other(s). In this work, with the aids of the solvent additive (1-chloronaphthalene) and the *n*-type polymer additive (N2200), we can fine-tune the morphology of the active layer and demonstrate a 16.04% efficient all-PSC based on the PM6:PY-IT active layer. The grazing incidence wide-angle X-ray scattering measurements show that the shape of the crystallites can be altered, and the reshaped crystallites lead to enhanced and more balanced charge transport, reduced recombination, and suppressed energy loss, which lead to concurrently improved and device efficiency and stability.

KEYWORDS

additive, all-polymer solar cell, energy loss, morphology, power conversion efficiency

Funding information
National Key Research and Development Program of China, Grant/Award Number: 2019YFA0705900; Basic and Applied Basic Research Major Program of Guangdong Province, Grant/Award Number: 2019B030302007; Guangdong-Hong Kong-Macao Joint Laboratory of Optoelectronic and Magnetic Functional Materials, Grant/Award Number: 2019B121205002; Shen Zhen Technology and Innovation Commission, Grant/Award Numbers: JCYJ20170413173814007, JCYJ20170818113905024; Hong Kong Research Grants Council (Research Impact Fund R6021-18; collaborative research fund C6023-19G, Grant/Award Numbers: 16309218, 16310019, 16303917; Hong Kong Innovation and Technology Commission, Grant/Award Numbers: ITC-CNERC14SC01, ITS/471/18; National Natural Science Foundation of China, Grant/Award Numbers: 21927811, 91433202; Swedish Research Council VR, Grant/Award Number: 2016-06146; Swedish Research Council and The Knut and Alice Wallenberg Foundation, Grant/Award Numbers: 2017.0186, 2016.0059; Hong Kong PhD Fellowship Scheme, Grant/Award Number: PF17-03929; Natural Science Foundation of Top Talent of SZTU, Grant/Award Number: 20200205; China Postdoctoral Science Foundation, Grant/Award Number: 2020M673054; Postdoctoral Fund of Jinan University, and National Natural Science Foundation of China, Grant/Award Number: 22005121

INTRODUCTION

All-polymer solar cells (all-PSCs) are considered as a promising photovoltaic technology due to their exclusive advantages. For instance, organic solar cells with all-polymer active layers can possess excellent stability and robustness together.[1–7] This type of photovoltaic has experienced two decades of slow development in terms of the power conversion efficiency (PCE) due to the lack of efficient polymeric materials. However, the recent practice of polymerized small molecular acceptors has brought the PCE of all-PSCs to a new level. There have been multiple reports with >10% PCEs within a short timeframe.[8–19] To date, the best performing all-PSCs demonstrate PCEs in the range of 15%–16%.[20–27] Nevertheless, compared to the achievements by the small molecule-based solar cells (~18% PCE), there is still a long way ahead for all-PSCs.[28–36]

From the experience of small molecule-based solar cells, fine-tuning the morphology and thus the device properties are essential for further improving the device efficiency in a material system that already manifests decent photovoltaic performance. In all-PSCs, it would be even more difficult because the formation of morphology is based on two tightly entangled materials both consisting of long conjugated chains. Particularly, it would be extremely challenging to improve all three main device parameters, that is, open-circuit voltage (V_{OC}), short-circuit current density (J_{SC}), and fill factor (*FF*) concurrently in the all-PSCs with advanced efficiency, and one increase is typically accompanied by the drop of the other(s). But this does not mean that there is no way to do this from the perspective of device engineering. For instance, the use of additives (solvents or solids, small molecules, or polymers) has been proven an effective strategy to promote the photovoltaic performances of solar cells, as reported by many.[37–42] In all-PSC systems, traditional solvent additives such as 1,8-diiodooctane (DIO) and 1-chloronaphthalene (CN) are also effective in promoting device performance. In addition to solvent additive, polymers are successfully used as additive in some recent cases as well. Min,[43] Yang,[44] and Huang[45] et al found that the use of polymer acceptor as additive could also efficiently enhance the device performance.

In this work, we employed the all-PSC based on PM6:PY-IT as the target system, which already demonstrated state-of-the-art photovoltaic performance,[21] and judiciously modified the morphology of the all-polymer active layer through fine-tuning the solvent additive and solid additive during film preparation for boosting device performance. Specifically, compared to the control device (1 *vol %* CN in active blend solution) with a PCE of 14.93%, we optimize the content of CN and utilize a small amount of N2200 as solid additive to fabricate all-PSC devices, which endow the devices with an excellent efficiency as high as 16.04%. The synergistic effect of the solvent and polymer additives improves the photovoltaic parameters of open-circuit voltage (V_{OC}), short-circuit current density (J_{SC}), and fill factor (*FF*) simultaneously. The grazing incidence wide-angle X-ray scattering (GIWAXS) and device physics studies show that the solvent and solid additives can effectively alter the shape of the crystallites, making them grow "taller" (relative to the substrate plane), then enhances the charge transport while suppressing recombination, which also leads to a reduced nonradiative voltage loss. Notably, compared to the control device, the optimal device with the aid of the solid additive also shows increased storage stability and photostability.

RESULTS AND DISCUSSION

The chemical structures of PM6, PY-IT, CN, and N2200 are shown in Figure 1A, and their optical properties, that is, the absorption in neat films and blend films, are shown

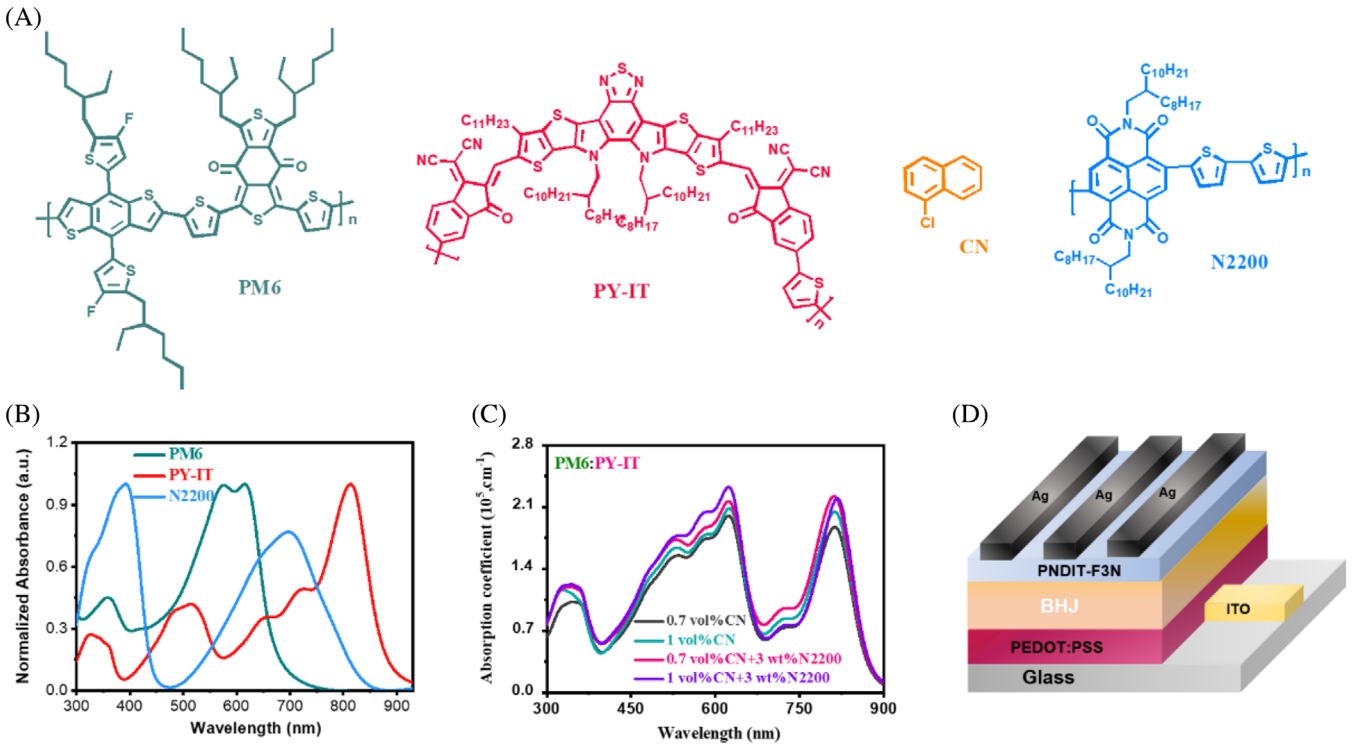

FIGURE 1 (A) Chemical structures. (B) Neat film and (C) blend film absorption spectra. (D) Device structure

TABLE 1 Photovoltaic parameters of APSCs

PM6:PY-IT	V_{OC} (V)	J_{SC} (mA·cm^{-2})	*FF* (%)	PCE (%)
Device I	(0.933 ± 0.003)[a] 0.936[b]	(21.30 ± 0.11) 21.41/21.35[c]	(73.1 ± 0.6) 73.6	(14.53 ± 0.11) 14.77
Device II	(0.930 ± 0.004) 0.932	(22.30 ± 0.12) 22.31/21.76	(71.5 ± 0.4) 71.8	(14.83 ± 0.10) 14.93
Device III	(0.943 ± 0.005) 0.947	(22.46 ± 0.11) 22.60/22.48	(74.6 ± 0.4) 74.9	(15.80 ± 0.12) 16.04
Device IV	(0.934 ± 0.003) 0.936	(22.77 ± 0.14) 22.92/22.75	(72.6 ± 0.5) 73.2	(15.44 ± 0.13) 15.72

[a]Values in brackets are average based on 20 independent devices.
[b]Values in this row are parameters associated with the devices that showed the highest PCEs.
[c]The integrated J_{SC} values from EQE spectra.

in Figures 1B and 1C, respectively. The complementarity between the absorption spectra of PM6 and PY-IT is clearly observed in Figure 1B, which is consistent with previous report. Besides, two main absorption peaks of N2200 are in the regions that are complementary to the absorption of the PM6:PY-IT blend film. N2200 used here is commercially available from 1-Materials; molecular weight is 30 KDa. Depending on the different amount of CN and/or N2200 used during solution/film preparation, we obtain four blend films that are all based on the same PM6:PY-IT: 0.7 *vol %* CN, 1 *vol %* CN, 0.7 *vol %* CN + 3 *wt %* N2200, and 1 *vol %* CN + 3 *wt %* N2200. Figure 1C shows the absorption spectra of these films. The main features are similar among them, but the film processed with 0.7 *vol %* CN and 3 *wt %* N2200 shows the highest absorption in the range of 680–750 nm. The absorption coefficients summarized in Table S1 include all details for comparison. In addition to absorption, we also evaluated the tendency of N2200 to mix with the PM6 and PY-IT through surface tension analysis (Figure S1). The result shows that surface tensions of PM6, PY-IT, and N2200 are 21.45, 20.98, and 21.50 N/m, respectively, which are close to each other, indicating a decent intermixing propensity of N2200 in the blend.[46–47]

Then we fabricated a series of devices using a structure of ITO/PEDOT:PSS/bulk heterojunction (BHJ)/PNDIT-F3N/Ag to study the effect of binary additives on the resulting solar cell performance. The current density *versus* voltage (*J-V*) characteristics of the devices are plotted in Figure 2A, and the corresponding photovoltaic parameters are listed in Table 1. The PM6:PY-IT-based binary all-PSC with 1 *vol%* CN (Device II) shows a PCE of 14.93%. By adding 3 *wt%* N2200 into the blend active layer (Device IV), the efficiency was promoted to as high as 15.72% owing to the simultaneously increased V_{OC}, J_{SC}, and *FF*. We find that fine-tuning the ratio of CN from 1 *vol%* to 0.7 *vol%* (Device I) allows us to improve the V_{OC} and *FF*, but the PCE is reduced to 14.77% due to the J_{SC} drop. To compensate the J_{SC} and thus increase all three parameters concurrently, we incorporated a small

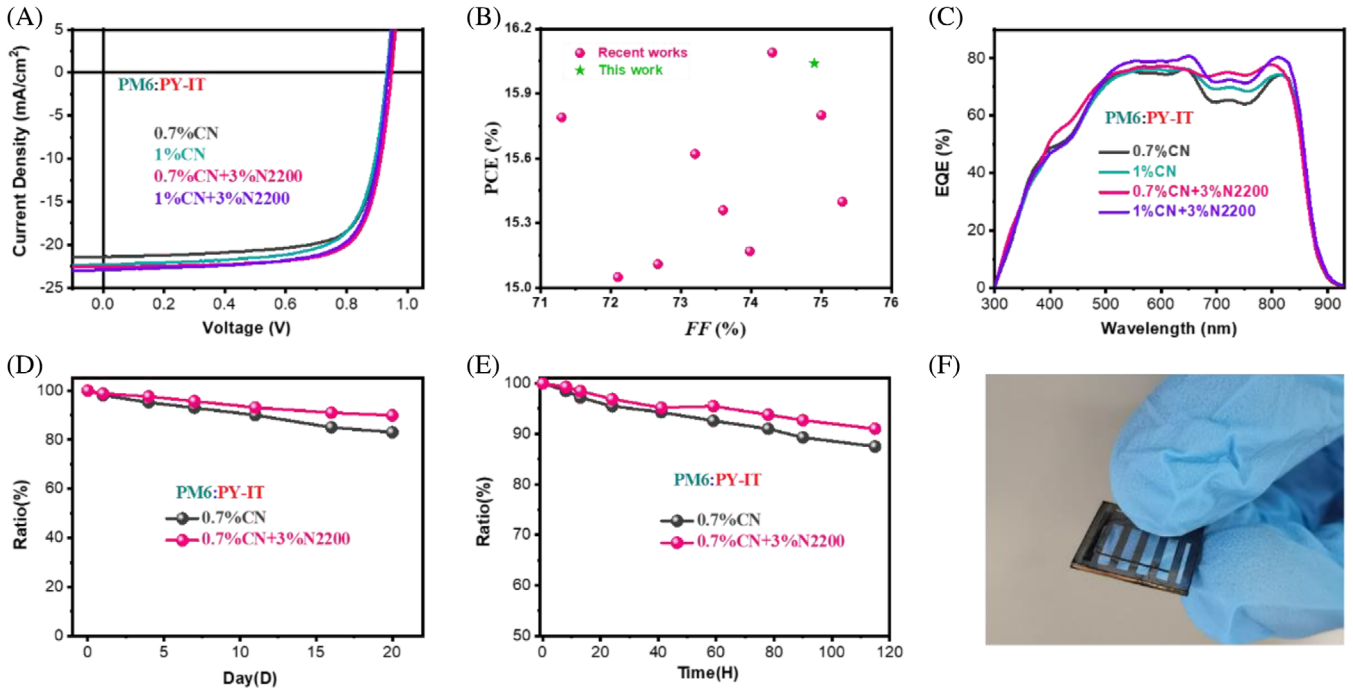

FIGURE 2 (A) *J-V* characteristics of PM6:PY-IT-based all-PSCs prepared using different amount of CN and N2200 as additives. (B) The PCE and FF of all-PSCs with >14% efficiency from literature along with this work. (C) The EQE spectra of devices. (D) Storage stability and (E) photostability of PM6:PY-IT-based devices with Device I and Device III. (F) A photo of the encapsulated device

amount of N2200 into the blend and examined the device performance influenced by the interplay between the solvent additive (CN) and the solid additive (N2200). We achieved the highest efficiency of 16.04% together with an excellent *FF* of 74.9% when 0.7 *vol%* CN and 3 *wt%* N2200 (Device III) were used. Notably, the PCE of 16.04% is the superior value for all-PSCs, regardless binary or ternary, single-junction, or tandem devices, to the best of our knowledge. Figure 2B summarizes the photovoltaic performance, *that is*, PCE versus *FF*, of recent all-PSCs with cutting-edge efficiencies (>15%), which highlights the significance of our results.

The external quantum efficiency (EQE) spectra of the devices are shown in Figure 2C. Comparing the J_{SC}s integrated from these EQE spectra and those from the *J-V* measurement (Table 1) shows that the errors are within 3%. Besides, the efficiency was confirmed by bringing them to another laboratory to test (Figure S2, supported by The Hong Kong Polytechnic University, Prof. Gang Li). Apart from efficiency, the device stability of all-PSCs is measured. The storage stability and photostability measurements for encapsulated devices pictured in Figure 2F were conducted in air conditions. We plot the change in efficiency with time in Figures 2D (storage stability) and 2E (light soaking), for Devices I and III. The T80 values for the latter are 997 and 250 h, for storage and light soaking stability, respectively,[48] where T80 means the time it costs for device to lose 20% of its initial PCE and was estimated by linear fitting. These results are significantly higher than those for Device I (557 and 194 h), demonstrating that the addition of N2200, despite a small amount, can reduce the decay of the devices. N2200 is supposed to be beneficial to thin film morphology stability of active layers, resulting better device stability. This method was successfully applied in some ternary works.[49–51] For storage stability test, the main differences of PCE degradation start from Day 10, indicating the original morphology of PM6:PY-IT was undergoing a more intensive degradation compared with N2200 doped film. This can also be the explanation of light soaking stability differences beginning from 40th h.

The addition of N2200 into the PM6:PY-IT blend leads to a further increased V_{OC} (from 0.932 to 0.947 V) relative to the device processed with CN as additive compared, which draws our interest since no significant blueshifts in absorption and EQE spectra are observed. This indicates that the inclusion of N2200 regulates the recombination and thus the energy loss (E_{loss}). To investigate the energy loss, we employed Fourier transform photocurrent spectroscopy EQE (FTPS-EQE) and electroluminescence EQE (EL-EQE). Figures 3A and 3B show the testing results of FTPS-EQE and EL-EQE, respectively. E_{loss} of a solar cell can be divided into three parts as described in the equation (details in supporting information):[52–53]

$$\begin{aligned} E_{loss} &= E_g - qV_{OC} = \left(E_g - qV_{OC}^{SQ}\right) + \left(qV_{OC}^{SQ} - qV_{OC}^{rad}\right) \\ &\quad + \left(qV_{OC}^{rad} - qV_{OC}\right) \\ &= \left(E_g - qV_{OC}^{SQ}\right) + q\Delta V_{OC}^{rad,below\ gap} + q\Delta V_{OC}^{non-rad} \\ &= \Delta E_1 + \Delta E_2 + \Delta E_3 \end{aligned}$$

ΔE_1 is an inevitable radiative loss for BHJ solar cells working under 1-sun or below, which can be calculated based on the Shockley-Queisser theory. The four PM6:PY-IT devices we studied in this work show the same value of ΔE_1 (0.27 eV); ΔE_2 is the radiative loss below the bandgap due to non-step-function like absorptance, which also appears to be identical (0.03 eV) for the devices in this work. The last part, ΔE_3, is the loss due to nonradiative recombination, which is quite different among different types of solar cells and can be calculated via $\Delta E_3 = -k_B T(\ln EQE_{EL})$, with k_B the Boltzmann

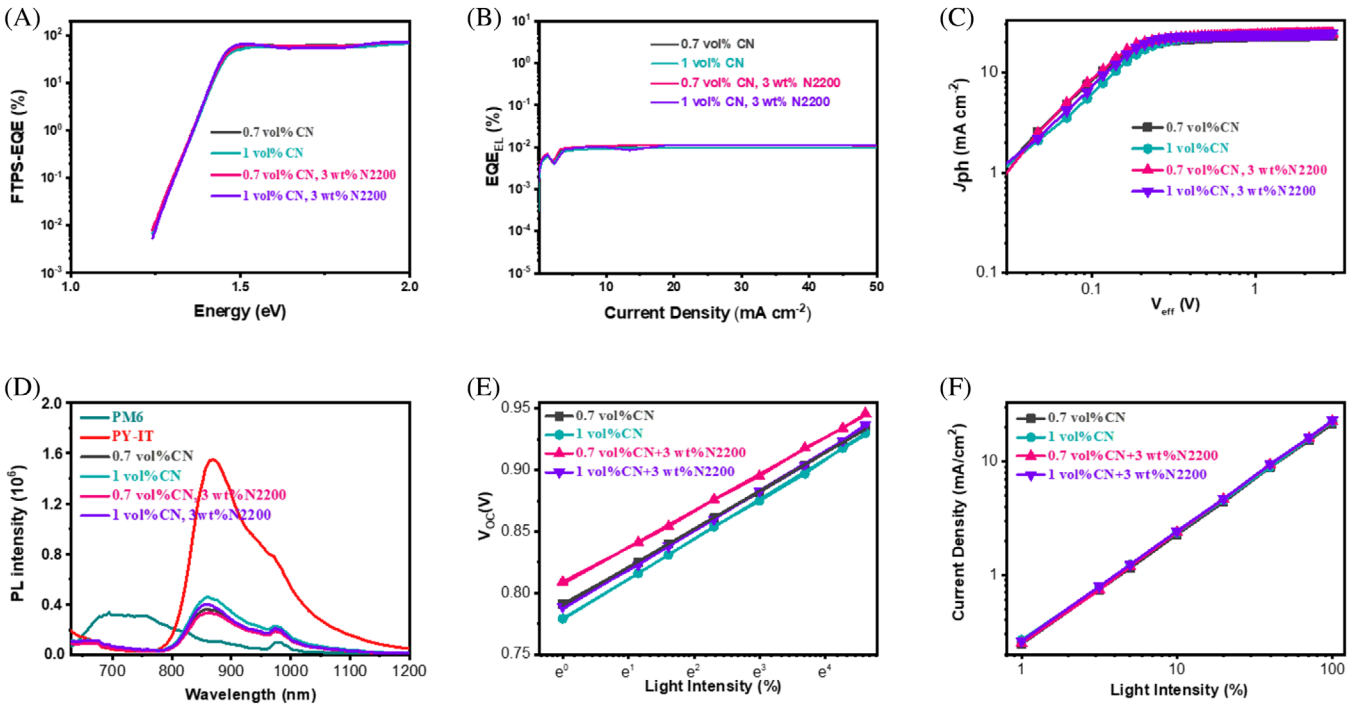

FIGURE 3 (A) FTPS-EQE and (B) EL-EQE spectra of devices. (C) J_{ph}-V_{eff} curves. (D) PL intensity of the neat films of PM6 and PY-IT and their blend films processed using different additive(s). (E) V_{OC} vs P_{light} and (F) J_{SC} vs P_{light} relationships

constant, T the absolute temperature, and EQE_{EL} the EQE of EL. Compared to the other three counterparts (0.24 V), Device III shows the smallest nonradiative recombination loss (0.23 V), the difference in which roughly matches the difference in the V_{OC} of their devices. This shows that the one of the combined efforts of 0.7 *vol%* CN and 3 *wt%* N2200 is reducing the nonradiative recombination.

In addition to V_{OC}, tuning the ratio of CN and adding N2200 also boosted the J_{SC} and *FF*. To understand the enhancement of these parameters, we first plot the photocurrent density (J_{ph}) as a function of the effective voltage (V_{eff}) (Figure 2C) to estimate the exciton dissociation (η_{diss}) and collection efficiency (η_{coll}).[54–56] J_{ph} is defined as the difference between the current density under illumination (J_L) and the dark current density (J_D). V_{eff} is the absolute value of V_0 - V_{appl}, where V_0 refers to the voltage when $J_L = J_D$, and V_{appl} is the applied voltage. At high V_{eff}, almost all excitons are separated and extracted, and J_{ph} reaches saturation (J_{sat}).η_{diss} and η_{coll} are defined by J_{SC}/J_{sat} and J_{max}/J_{sat}, respectively, in which J_{max} is the current density at the maximal output point. (η_{diss}, η_{coll})s of all-PSCs we focus on are (92.8%, 82.1%), (91.6%, 78.5%), (93.3%, 83.7%), and (92.5%, 80.3%) for 0.7 *vol%* CN, 1 *vol%* CN, 0.7 *vol%* CN & 3 *wt%* N2200, and 1 *vol%* CN & 3 *wt%* N2200 treated blends, respectively. This trend agrees with the trend of the *FF* of their devices. Next, we measured the steady-state photoluminescence (PL) spectra of the polymer neat film and the blend films (Figure 2D) to compare the quenching efficiency.[57–59] The PL quenching efficiencies are 74.1% for the Device I, 70.3% for Device II, 78.2% for Device III, and 76.3% for Device IV, consistent with analysis above.

Furthermore, we measured the *J-V* characteristics of the devices under different light intensities to study the change in recombination.[60–61] Figure 2E delivers the relationship between J_{SC} and light intensity (P_{light}), and Figure **2F** shows that between V_{OC} and P_{light}. Theoretically, V_{OC} is linearly proportional to ln(P_{light}), and the slope is equal to nkT/q, where n is the ideality factor, k is the Boltzmann constant, T is the temperature, and q is the elementary charge. Fitting the data in Figure 2E provides us with the values of the ideality factor, which are 1.197, 1.254, 1.147, and 1.236 for Device I, II, III, and IV, respectively, also consistent with the trend of the FF. This implies that the trap-assisted recombination and monomolecular recombination are least dominant in the optimal active layer (Device III). To assess the bimolecular recombination, we fit the curves of J_{SC} versus ln(P_{light}). The slope from the fitting (S) is theoretically less than 1, and the closer it is to unity, the weaker the bimolecular recombination is in the device. The S values from fitting the data in Figure 2F are 0.972, 0.960, 0.983, and 0.972 for Device I, II, III, and IV, respectively, suggesting that our best device also has the weakest bimolecular recombination.

Based on electrical characterization and recombination analysis, we then turn our attention to the morphology of the active layer as it is directly related to the processing solvents and materials composition during film preparation. We first performed atomic force microscopy measurements on the films of the four blends (Figure S3), which show similar surface morphology. We then carried out GIWAXS experiments.[62–64] The 2D patterns of the blend films are demonstrated in Figure 4A, while the corresponding intensity profiles in the in-plane (IP) and out-of-plane (OOP) directions are shown in Figure 4B. The peaks corresponding to the lamellar packing of all four blends are located at 0.30 $Å^{-1}$, and the intensity is in the IP direction, but the crystalline coherent lengths (CCLs) are 50.0, 58.3, 40.9, and 54.9 Å for Device I, II, III, and IV, respectively. The π-π stacking peaks, found in the OOP direction, are all located at 1.67–1.68 $Å^{-1}$. In contrast to the CCL of the lamellar packing, the CCLs for the π-π stacking peaks in the OOP direction

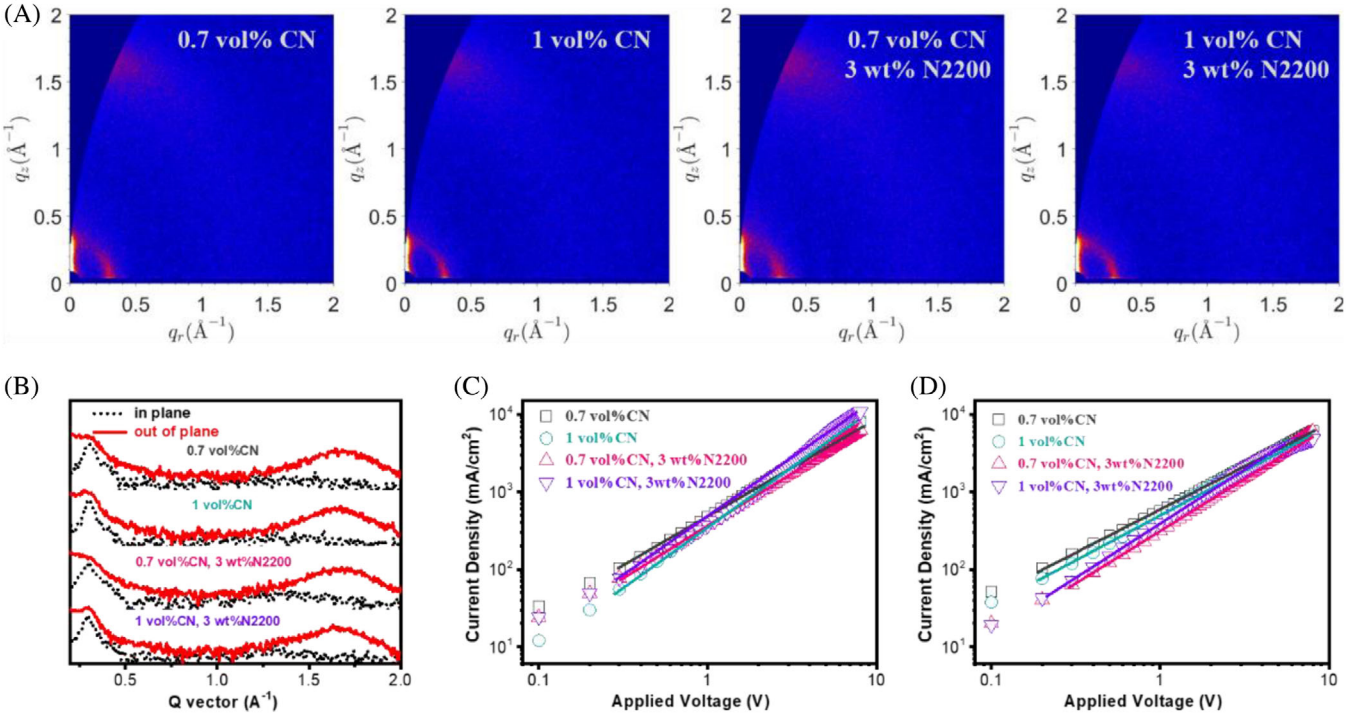

FIGURE 4 (A) 2D GIWAXS patterns. (B) Line-cut profiles in the in-plane and out-of-plane direction. (C) Hole-only and (D) electron-only device results

are 20.4, 19.1, 23.8, and 19.7 Å, for Device I, II, III and IV, respectively. These data suggest that either using less CN or adding N2200 into the blend can suppress the IP lamellar packing while promote π-π stacking. In other words, the combined effect of the optimized amount of CN and N2200 is to alter the shape of the crystallites, reducing the initially overly packed lamellar while enhancing the π-π stacking in the OOP direction, rendering "taller" and face-on crystallites. To figure out N2200's role in thin film morphology tuning, we evaluated the neat film GIWAXS results for PM6, PY-IT, and N2200 (Figure S4). PM6 exhibits a (100) peak at 0.29 Å^{-1} alongside IP direction, whose CCL is 59.5 Å, meanwhile a (010) peak of 1.72 Å^{-1} with a 17.66 Å CCL in OOP orientation. PY-IT displays a lamellar peak ~ 0.38 Å^{-1} (CCL = 43.4 Å) on IP direction, and an OOP located π-π stacking peak (q ~ 1.65 Å^{-1}) with 18.84 Å CCL. These two material-merged blend films demonstrate reasonable molecular packing features as described above. In contrast, N2200 contains two IP peaks at 0.26 and 0.47 Å^{-1}, which might undermine the IP packing through doping. Furthermore, the (010) peak with strong intensity can be beneficial to OOP orientated π-π stacking. This should benefit to charge transport in the active layer as the vertical charge transport is the desired pathway for charge extraction. To investigate the effect of such morphology change, we fabricate hole-only (Figure 4C) and electron-only (Figure 4D) devices and measure the *J-V* characteristics to evaluate the charge carrier mobilities. The hole (μ_h) and electron mobility (μ_e) fitted using the space-charge limited current (SCLC) model are 8.23 and 4.63 × 10^{-4} cm^2 V^{-1} s^{-1} for Device I, with a hole/electron mobility ratio (μ_h/μ_e) of 1.78. In comparison, the μ_h and μ_e for Device II are 7.61 and 4.55 × 10^{-4} cm^2 V^{-1} s^{-1}, and the μ_h/μ_e is 1.67, which indicates that reducing the CN ratio leads to slightly lowered mobilities but more balanced hole charge transport. Besides, μ_h for Device III and Device IV are 8.79 and 7.98 × 10^{-4} cm^2 V^{-1} s^{-1}, while the μ_e for are 5.22 and 4.89 × 10^{-4} cm^2 V^{-1} s^{-1}, respectively. Therefore, the overall result of CN and N2200 is enhancing hole and electron transport simultaneously, and balancing them in the meantime, which is consistent with the morphology result and the J_{SC}, *FF* of the devices.

CONCLUSION

In summary, we combined the polymer additive, N2200, with the solvent additive, CN, during film preparation of the PM6:PY-IT-based all-PSCs, which improved the PCE from 14.93% to 16.04%, the highest value for this kind photovoltaics. Reduced nonradiative loss, more efficient charge generation, and lower recombination were enabled by fine-tuning the proportion of additives, which led to concurrently promoted V_{OC}, J_{SC} and *FF*. Morphology study revealed that these improved photovoltaic performances are correlated with the change in the crystallite molecular packing, *i.e.*, from a "wide and short" shape to a "narrower but taller" form, which increased and balanced charge transport. Besides, optimized devices show enhanced stability compared to the control device, exhibiting T80 values as high as 997 and 250 h for storage and light soaking stability, which are also at cutting-edge level for state-of-the-art polymerized small molecular acceptor-based all-PSCs. Overall, this work successfully pushed the efficiency of all-PSCs up to > 16%, which strongly enhances the competitiveness of this device platform.

ACKNOWLEDGMENT

This work is supported by the National Key Research and Development Program of China (number: 2019YFA0705900) funded by MOST, the Basic and Applied

Basic Research Major Program of Guangdong Province (number: 2019B030302007), Guangdong-Hong Kong-Macao Joint Laboratory of Optoelectronic and Magnetic Functional Materials (project number: 2019B121205002), the Shen Zhen Technology and Innovation Commission (project numbers: JCYJ20170413173814007 and JCYJ20170818113905024), the Hong Kong Research Grants Council (Research Impact Fund R6021-18, collaborative research fund C6023-19G, project numbers: 16309218, 16310019, and 16303917), Hong Kong Innovation and Technology Commission for the support through projects ITC-CNERC14SC01 and ITS/471/18), National Natural Science Foundation of China (NSFC, number: 91433202). Bo Tang thanks the financial support from National Natural Science Foundation of China 21927811. Feng Gao acknowledges the financial support from the Swedish Research Council VR (2016-06146). Ergang Wang thanks the Swedish Research Council and The Knut and Alice Wallenberg Foundation (2017.0186, 2016.0059). Guangye Zhang appreciates the support from Natural Science Foundation of Top Talent of SZTU (grant number: 20200205). Ruijie Ma acknowledges the support from Hong Kong PhD Fellowship Scheme PF17-03929. Wenyan Su thanks the project funded by China Postdoctoral Science Foundation (2020M673054), Postdoctoral Fund of Jinan University, and National Natural Science Foundation of China (22005121). We appreciate Prof. Gang Li, Dr. Cenqi Yan and Dr. Jiangsheng Yu for aiding in efficiency confirmation.

CONFLICT OF INTEREST

The authors declare no conflict of interest.

AUTHOR CONTRIBUTION

Ruijie Ma proposed the idea. Ruijie Ma fabricated devices. Jianwei Yu and Feng Gao tested energy loss. Yiqun Xiao and Xinhui Lu did GIWAXS/SAXS experiments. Zhenghui Luo and Gaoda Chai provided the materials. Qunping Fan and Ergang Wang delivered important academic suggestions. Yuzhong Chen, Wenyan Su, and Gang Li helped with basic characterizations. Ruijie Ma drafted the manuscript. Guangye Zhang revised the paper. Tao Liu, Guangye Zhang, Feng Gao, He Yan, and Bo Tang supervised the project.

ORCID

Ruijie Ma https://orcid.org/0000-0002-7227-5164
Bo Tang https://orcid.org/0000-0002-8712-7025

REFERENCES

1. C. Lee, S. Lee, G.-U. Kim, W. Lee, B. J. Kim, *Chem. Rev.* **2019**, *119*, 8028.
2. G. Wang, F. S. Melkonyan, A. Facchetti, T. J. Marks, *Angew. Chem. Int. Ed.* **2019**, *58*, 4129.
3. Y. Lin, S. Dong, Z. Li, W. Zheng, J. Yang, A. Liu, W. Cai, F. Liu, Y. Jiang, T. P. Russell,, E. Wang, L. Hou, *Nano Energy* **2018**, *46*, 428.
4. J.-W. Lee, C. Sun, B. S. Ma, H. J. Kim, C. Wang, J. M. Ryu, C. Lim, T.-S. Kim, Y.-H. Kim, S.-K. Kwon, B. J. Kim, *Adv. Energy Mater.* **2020**, *11*, 2003367.
5. Y. Xu, J. Yuan, S. Liang, J.-D. Chen, Y. Xia, B. W. Larson, Y. Wang, G. M. Su, Y. Zhang, C. Cui, M. Wang, H. Zhao, W. Ma, *ACS Energy Lett.* **2019**, *4*, 2277.
6. J. W. Jung, J. W. Jo, C.-C. Chueh, F. Liu, W. H. Jo, T. P. Russell, A. K.-Y. Jen, *Adv. Mater.* **2015**, *27*, 3310.
7. S. Chen, S. Jung, H. J. Cho, N.-H. Kim, S. Jung, J. Xu, J. Oh, Y. Cho, H. Kim, B. Lee, Y. An, C. Zhang, M. Xiao, H. Ki, Z.-G. Zhang, J.-Y. Kim, Y. Li, H. Park, C. Yang, *Angew. Chem. Int. Ed.* **2018**, *57*, 13277.
8. R. Zhao, J. Liu, L. Wang, *Acc. Chem. Res.* **2020**, *53*, 1557.
9. L. Zhu, W. Zhong, C. Qiu, B. Lyu, Z. Zhou, M. Zhang, J. Song, J. Xu, J. Wang, J. Ali, W. Feng, Z. Shi, X. Gu, L. Ying, Y. Zhang, F. Liu, *Adv. Mater.* **2019**, *31*, 1902899.
10. H. Chen, Y. Guo, P. Chao, L. Liu, W. Chen, D. Zhao, F. He, *Sci. China Chem.* **2019**, *62*, 238.
11. H. Sun, B. Liu, J. Yu, X. Zou, G. Zhang, Y. Zhang, W. Zhang, M. Su, Q. Fan, K. Yang, J. Chen, H. Yan, F. Gao, X. Guo, *Sci. China Chem.* **2020**, *63*, 1785.
12. N. B. Kolhe, D. K. Tran, H. Lee, D. Kuzuhara, N. Yoshimoto, T. Koganezawa, S. A. Jenekhe, *ACS Energy Lett*. **2019**, *4*, 1162.
13. P. Cheng, L. Ye, X. Zhao, J. Hou, Y. Li, X. Zhan, *Energy Environ. Sci.* **2014**, *7*, 1351.
14. Z.-G. Zhang, Y. Li, *Angew. Chem. Int. Ed.* **2020**, *60*, 4422.
15. Q. Fan, W. Su, S. Chen, T. Liu, W. Zhuang, R. Ma, X. Wen, Z. Yin, Z. Luo, X. Guo, L. Hou, K. Moth-Poulsen, Y. Li, Z. Zhang, C. Yang, D. Yu, H. Yan, M. Zhang, E. Wang, *Angew. Chem. Int. Ed.* **2020**, *59*, 19835.
16. J. Du, K. Hu, L. Meng, I. Angunawela, J. Zhang, S. Qin, A. Liebman-Pelaez, C. Zhu, Z. Zhang, H. Ade, Y. Li, *Angew. Chem. Int. Ed.* **2020**, *59*, 15181.
17. J. Wu, Y. Meng, X. Guo, L. Zhu, F. Liu, M. Zhang, *J. Mater. Chem. A* **2019**, *7*, 16190.
18. Q. Wu, W. Wang, T. Wang, R. Sun, J. Guo, Y. Wu, X. Jiao, C. J. Brabec, Y. Li, J. Min, *Sci. China Chem.* **2020**, *63*, 1449.
19. Q. Fan, R. Ma, T. Liu, W. Su, W. Peng, M. Zhang, Z. Wang, X. Wen, Z. Cong, Z. Luo, L. Hou, F. Liu, W. Zhu, D. Yu, H. Yan, E. Wang, *Solar RRL* **2020**, *4*, 2000142.
20. T. Jia, J. Zhang, K. Zhang, H. Tang, S. Dong, C.-H. Tan, X. Wang, F. Huang, *J. Mater. Chem. A* **2021**, *9*, 8975.
21. Z. Luo, T. Liu, R. Ma, Y. Xiao, L. Zhan, G. Zhang, H. Sun, F. Ni, G. Chai, J. Wang, C. Zhong, Y. Zou, X. Guo, X. Lu, H. Chen, H. Yan, C. Yang, *Adv. Mater.* **2020**, *32*, 2005942.
22. Q. Wu, W. Wang, Y. Wu, Z. Chen, J. Guo, R. Sun, J. Guo, Y. Yang, J. Min, *Adv. Funct. Mater* **2021**, *30*, 2010411.
23. F. Peng, K. An, W. Zhong, Z. Li, L. Ying, N. Li, Z. Huang, C. Zhu, B. Fan, F. Huang, Y. Cao, *ACS Energy Lett*. **2020**, *5*, 3702.
24. L. Zhang, T. Jia, L. Pan, B. Wu, Z. Wang, K. Gao, F. Liu, C. Duan, F. Huang, Y. Cao, *Sci. China Chem.* **2021**, *64*, 408.
25. H. Fu, Y. Li, J. Yu, Z. Wu, Q. Fan, F. Lin, H. Y. Woo, F. Gao, Z. Zhu, A. K. Y. Jen, *J. Am. Chem. Soc* **2021**, *143*, 2665.
26. R. Ma, M. Zeng, Y. Li, T. Liu, Z. Luo, Y. Xu, P. Li, N. Zheng, J. Li, Y. Li, R. Chen, J. Hou, F. Huang, H. Yan, *Adv. Energy Mater.* **2021**, *n/a*, 2100492. https://doi.org/10.1002/aenm.202100492
27. T. Liu, T. Yang, R. Ma, L. Zhan, Z. Luo, G. Zhang, Y. Li, K. Gao, Y. Xiao, J. Yu, X. Zou, H. Sun, M. Zhang, T. A. Dela Peña, Z. Xing, H. Liu, X. Li, G. Li, J. Huang, C. Duan, K. S. Wong, X. Lu, X. Guo, F. Gao, H. Chen, F. Huang, Y. Li, Y. Li, Y. Cao, B. Tang, H. Yan, *Joule* **2021**. https://doi.org/10.1016/j.joule.2021.02.002.
28. K. Jin, Z. Xiao, L. Ding, *J. Semicond.* **2021**, *42*, 010502.
29. M. Zhang, L. Zhu, G. Zhou, T. Hao, C. Qiu, Z. Zhao, Q. Hu, B. W. Larson, H. Zhu, Z. Ma, Z. Tang, W. Feng, Y. Zhang, T. P. Russell, F. Liu, *Nat. Commun.* **2021**, *12*, 309.
30. R. Ma, T. Liu, Z. Luo, K. Gao, K. Chen, G. Zhang, W. Gao, Y. Xiao, T.-K. Lau, Q. Fan, Y. Chen, L.-K. Ma, H. Sun, G. Cai, T. Yang, X. Lu, E. Wang, C. Yang, A. K. Y. Jen, H. Yan, *ACS Energy Lett*. **2020**, *5*, 2711.
31. J. Wu, G. Li, J. Fang, X. Guo, L. Zhu, B. Guo, Y. Wang, G. Zhang, L. Arunagiri, F. Liu, H. Yan, M. Zhang, Y. Li, *Nat. Commun.* **2020**, *11*, 4612.
32. Q. Liu, Y. Jiang, K. Jin, J. Qin, J. Xu, W. Li, J. Xiong, J. Liu, Z. Xiao, K. Sun, S. Yang, X. Zhang, L. Ding, *Sci. Bull.* **2020**, *65*, 272.
33. L. Zhan, S. Li, X. Xia, Y. Li, X. Lu, L. Zuo, M. Shi, H. Chen, *Adv. Mater.* **2021**, *33*, 2007231.
34. X. Ma, A. Zeng, J. Gao, Z. Hu, C. Xu, J. H. Son, S. Y. Jeong, C. Zhang, M. Li, K. Wang, H. Yan, Z. Ma, Y. Wang, H. Y. Woo, F. Zhang, *Natl. Sci. Rev.* **2020**. https://doi.org/10.1093/nsr/nwaa305.
35. X. Xu, L. Yu, H. Yan, R. Li, Q. Peng, *Energy Environ. Sci.* **2020**, *13*, 4381.
36. Q. Kang, Z. Zheng, Y. Zu, Q. Liao, P. Bi, S. Zhang, Y. Yang, B. Xu, J. Hou, *Joule* **2021**, *5*, 646.

37. T. Kumari, S. Jung, Y. Cho, H.-P. Kim, J. W. Lee, J. Oh, J. Lee, S. M. Lee, M. Jeong, J. M. Baik, W. Jo, C. Yang, *Nano Energy* **2020**, *68*, 104327.
38. L. Liu, Y. Kan, K. Gao, J. Wang, M. Zhao, H. Chen, C. Zhao, T. Jiu, A.-K. Y. Jen, Y. Li, *Adv. Mater.* **2020**, *32*, 1907604.
39. L. Ye, Y. Cai, C. Li, L. Zhu, J. Xu, K. Weng, K. Zhang, M. Huang, M. Zeng, T. Li, E. Zhou, S. Tan, X. Hao, Y. Yi, F. Liu, Z. Wang, X. Zhan, Y. Sun, *Energy Environ. Sci.* **2020**, *13*, 5117.
40. X. Wang, A. Tang, J. Yang, M. Du, J. Li, G. Li, Q. Guo, E. Zhou, *Sci. China Chem.* **2020**, *63*, 1666.
41. R. Yu, H. Yao, L. Hong, Y. Qin, J. Zhu, Y. Cui, S. Li, J. Hou, *Nat. Commun.* **2018**, *9*, 4645.
42. K. Schmidt, C. J. Tassone, J. R. Niskala, A. T. Yiu, O. P. Lee, T. M. Weiss, C. Wang, J. M. J. Fréchet, P. M. Beaujuge, M. F. Toney, *Adv. Mater.* **2014**, *26*, 300.
43. W. Yang, Z. Luo, R. Sun, J. Guo, T. Wang, Y. Wu, W. Wang, J. Guo, Q. Wu, M. Shi, H. Li, C. Yang, J. Min, *Nat. Commun.* **2020**, *11*, 1218.
44. S. Dong, K. Zhang, T. Jia, W. Zhong, X. Wang, F. Huang, Y. Cao, *EcoMat* **2019**, *1*, e12006.
45. T. Yang, R. Ma, H. Cheng, Y. Xiao, Z. Luo, Y. Chen, S. Luo, T. Liu, X. Lu, H. Yan, *J. Mater. Chem. A* **2020**, *8*, 17706.
46. Y. Lin, M. I. Nugraha, Y. Firdaus, A. D. Scaccabarozzi, F. Aniés, A.-H. Emwas, E. Yengel, X. Zheng, J. Liu, W. Wahyudi, E. Yarali, H. Faber, O. M. Bakr, L. Tsetseris, M. Heeney, T. D. Anthopoulos, *ACS Energy Lett*. **2020**, *5*, 3663.
47. R. Ma, G. Li, D. Li, T. Liu, Z. Luo, G. Zhang, M. Zhang, Z. Wang, S. Luo, T. Yang, F. Liu, H. Yan, B. Tang, *Solar RRL* **2020**, *4*, 2000250.
48. Z. Jiang, F. Wang, K. Fukuda, A. Karki, W. Huang, K. Yu, T. Yokota, K. Tajima, T.-Q. Nguyen, T. Someya, *Proc. Natl. Acad. Sci.* **2020**, *117*, 6391.
49. N. Zheng, K. Mahmood, W. Zhong, F. Liu, P. Zhu, Z. Wang, B. Xie, Z. Chen, K. Zhang, L. Ying, F. Huang, Y. Cao, *Nano Energy* **2019**, *58*, 724.
50. Q. An, F. Zhang, W. Gao, Q. Sun, M. Zhang, C. Yang, J. Zhang, *Nano Energy* **2018**, *45*, 177.
51. H. Yin, K. L. Chiu, P. Bi, G. Li, C. Yan, H. Tang, C. Zhang, Y. Xiao, H. Zhang, W. Yu, H. Hu, X. Lu, X. Hao, S. K. So, *Adv. Electron. Mater.* **2019**, *5*, 1900497.
52. D. P. Qian, Z. L. Zheng, H. F. Yao, W. Tress, T. R. Hopper, S. L. Chen, S. S. Li, J. Liu, S. S. Chen, J. B. Zhang, X. K. Liu, B. W. Gao, L. Q. Ouyang, Y. Z. Jin, G. Pozina, I. A. Buyanova, W. M. Chen, O. Inganas, V. Coropceanu, J. L. Bredas, H. Yan, J. H. Hou, F. L. Zhang, A. A. Bakulin, F. Gao, *Nat. Mater.* **2018**, *17*, 703.
53. Y. Wang, D. Qian, Y. Cui, H. Zhang, J. Hou, K. Vandewal, T. Kirchartz, F. Gao, *Adv. Energy Mater.* **2018**, *8*, 1801352.
54. A. Karki, J. Vollbrecht, A. L. Dixon, N. Schopp, M. Schrock, G. N. M. Reddy, T.-Q. Nguyen, *Adv. Mater.* **2019**, *31*, 1903868.
55. R. Ma, T. Liu, Z. Luo, Q. Guo, Y. Xiao, Y. Chen, X. Li, S. Luo, X. Lu, M. Zhang, Y. Li, H. Yan, *Sci. China Chem.* **2020**, *63*, 325.
56. C. e. Zhang, S. Ming, H. Wu, X. Wang, H. Huang, W. Xue, X. Xu, Z. Tang, W. Ma, Z. Bo, *J. Mater. Chem. A* **2020**, *8*, 22907.
57. A. Classen, C. L. Chochos, L. Lüer, V. G. Gregoriou, J. Wortmann, A. Osvet, K. Forberich, I. McCulloch, T. Heumüller, C. J. Brabec, *Nat. Energy* **2020**, *5*, 711.
58. G. Liu, J. Jia, K. Zhang, X. e. Jia, Q. Yin, W. Zhong, L. Li, F. Huang, Y. Cao, *Adv. Energy Mater.* **2019**, *9*, 1803657.
59. S. Hultmark, S. H. K. Paleti, A. Harillo, S. Marina, F. A. A. Nugroho, Y. Liu, L. K. E. Ericsson, R. Li, J. Martín, J. Bergqvist, C. Langhammer, F. Zhang, L. Yu, M. Campoy-Quiles, E. Moons, D. Baran, C. Müller, *Adv. Funct. Mater.* **2020**, *30*, 2005462.
60. M. A. Adil, J. Zhang, Y. Wang, J. Yu, C. Yang, G. Lu, Z. Wei, *Nano Energy* **2020**, *68*, 104271.
61. A. Karki, J. Vollbrecht, A. J. Gillett, P. Selter, J. Lee, Z. Peng, N. Schopp, A. L. Dixon, M. Schrock, V. Nádaždy, F. Schauer, H. Ade, B. F. Chmelka, G. C. Bazan, R. H. Friend, T.-Q. Nguyen, *Adv. Energy Mater.* **2020**, *10*, 2001203.
62. B. A. Collins, Z. Li, J. R. Tumbleston, E. Gann, C. R. McNeill, H. Ade, *Adv. Energy Mater.* **2013**, *3*, 65.
63. T. Liu, Y. Zhang, Y. Shao, R. Ma, Z. Luo, Y. Xiao, T. Yang, X. Lu, Z. Yuan, H. Yan, Y. Chen, Y. Li, *Adv. Funct. Mater.* **2020**, *30*, 2000456.
64. R. Wang, S.-Y. Chang, L. Meng, W. Huang, J.-W. Lee, H.-W. Cheng, T. Huang, Y. Liu, J. Xue, P. Sun, C. Zhu, P. Cheng, Y. Yang, *Matter* **2019**, *1*, 402.

SUPPORTING INFORMATION

Additional supporting information may be found online in the Supporting Information section at the end of the article.

How to cite this article: R. Ma, J. Yu, T. Liu, G. Zhang, Y. Xiao, Z. Luo, G. Chai, Y. Chen, Q. Fan, W. Su, G. Li, E. Wang, X. Lu, F. Gao, H. Yan, B. Tang. *Aggregate*. **2021**, e58. https://doi.org/10.1002/agt2.58